Computing the attenuation of airborne sound in double-panelled constructions (without coupling between panels)

Gosele, K.

Publisher's version / Version de l'éditeur:
https://doi.org/10.4224/20338220
Technical Translation (National Research Council Canada); no. TT-2000, 1981

NATIONAL RESEARCH COUNCIL OF CANADA
CONSEIL NATIONAL DE RECHERCHES DU CANADA

TECHNICAL TRANSLATION 2000
TRADUCTION TECHNIQUE

Author/Auteur:	K. Gösele
Title/Titre:	Computing the Attenuation of Airborne Sound in Double-Panelled Constructions (Without Coupling Between Panels)
Reference/Référence:	Acustica, vol. 45 (1980)
Translator/Traducteur:	Peter Hessel

Canada Institute for Scientific and Technical Information

Institut canadien de l'information scientifique et technique

Ottawa, Canada
K1A 0S2

PREFACE

The Division of Building Research has been studying sound transmission through partitions for many years as part of its program to assess noise problems in multi-family dwellings. Although test measurements have been made for many types of partitions and some empirical prediction procedures have been devised, no fully satisfactory general theoretical treatment of the subject has developed. Many approaches to specific aspects of the problem have been reported and the extensive work by German investigators has been consistently in the forefront of this field. This translation of a paper from a German journal presents a simple method for predicting sound transmission through double-layered constructions with particular attention to effects of the stiffness of the medium in the interpanel cavity.

The Division of Building Research is grateful to Mr. P. Hessel for translating the paper and to Dr. J.D. Quirt of this Division who checked the translation.

Ottawa,
February, 1981

C.B. Crawford,
Director.

COMPUTING THE ATTENUATION OF AIRBORNE SOUND IN DOUBLE-PANELLED CONSTRUCTIONS (WITHOUT COUPLING BETWEEN PANELS)

by K. Gösele*

Summary

The study describes a simple method for approximating the attenuation of airborne sound in double-panelled constructions. Starting point is a "mass-spring-mass" model patterned after Wintergerst, but using reduced masses instead of true area-related masses. The reduced masses were selected in such a way that as single panels they result in the same attenuation of sound as computed or experimental attenuation for the wall panel in question. Apart from the frequency range directly adjacent to the critical frequency of the panels, there is good agreement between computed and experimental results. An important conclusion is that the resonance frequency of double walls consisting of stiff panels is 3 to 5 times higher that has hitherto been assumed.

1. Introduction

One of the most important measures to improve the attenuation of airborne sound in partitions, ceilings, doors, etc. consists in designing such constructions with two panels. It is therefore surprising that thus far no reliable method exists for computing the attenuation of airborne sound in such constructions. There are several studies dealing with this problem such as Wintergerst (1), London (2), etc.

However, these computed results do not give sufficient agreement with experiment; cf. Cops et al (3). In the present study we demonstrate an approximation method which is then compared with the experimental results from double panelled walls of greatly varying design. The computation is limited to a case in which sound is transmitted only via the insulation or air layer between panels, where the air layer is provided with an aerodynamic resistance, such as

* Author's address: Grundstrasse 32
D-7022 Leinfelden-Echterdingen 3
Federal Republic of Germany

mineral wool. This computation does not take into account the effect of solid couplings between panels, or the effect of possible flanking transmission via lateral constructions. /p. 219

2. Computation based on an extended two-mass model

2.1 Previous model

A long time ago, E. Wintergerst (1) demonstrated the principle of double-panelled walls by means of a simple model (Fig. 1), in which two masses, m_1' and m_2', were connected with each other via a spring of stiffness s'.

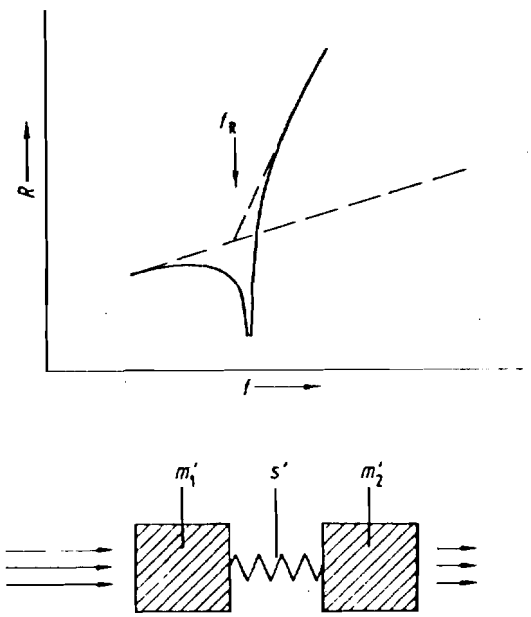

Fig. 1. Acoustic model of a double-panelled wall, after Wintergerst (1), and the resulting path of the attenuation factor R.

It is assumed that mass m_1' is excited by means of airborne sound. Thus, the resulting attenuation factor R for vertical sound incidence (see, for example, equations 1 and 3) above f_R is:

$$R = 20 \lg \left[\frac{\pi f m_1'}{\varrho c}\right] + 20 \lg \left[\frac{\pi f m_2'}{\varrho c}\right] + 20 \lg \left[\frac{4 \pi \cdot f \cdot \varrho c}{s'}\right] \text{dB} \qquad (1)$$

$$f_R = \frac{1}{2\pi} \sqrt{s' \left(\frac{1}{m_1'} + \frac{1}{m_2'}\right)}, \qquad (2)$$

in which

m_1': area-related mass of panel 1,
m_2': area-related mass of panel 2,
s' : area-related stiffness of the insulation layer,
ϱ : air density,
c : velocity of sound in air,
f : frequency,
f_R : resonance frequency of the arrangement.

This model represents very well the qualitative characteristics of a double wall, namely the occurrence of a resonance frequency f_R and the sharp increase in attenuation above f_R (cf. diagram in Fig. 1). However, quantitative agreement is unsatisfactory, particularly in the case of stiff, heavy panels. Deviations between computed and experimental values for stiff panels are shown in an example in Fig. 2; they are in the 20 - 40 dB range, depending on frequency. The reason for the deviations is obvious. The model assumes a vertical sound incidence and takes into account only the mass inertia of the panels and not their bending stiffness. Since Cremer's studies (10) it has been known that because of bending stiffness in stiff panels with obliquely incident sound the attenuation is 10-20 dB less above the critical frequency. Since deviations between the behaviour of actual panels and the above model occur even in the case of single panels, it is understandable that they occur even more frequently in double walls.

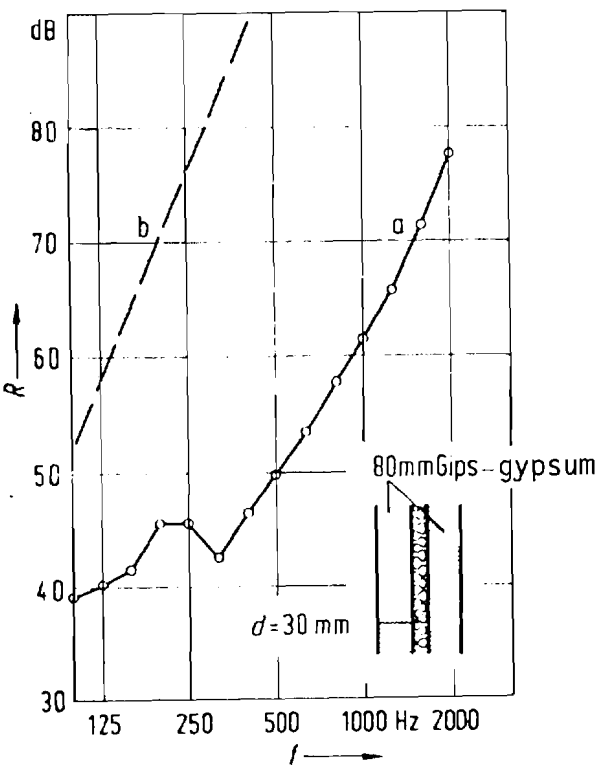

Fig. 2. Deviation between experimental results (curve a) and computed results, according to the original Wintergerst model, Fig. 1 (curve b) in a double wall made of stiff panels.

2.2 Improved model

/p.220

Below an attempt is made to maintain the model in principle but to modify it in as much as the vibrating (area-related) masses m_1' and m_2' are not assumed to equal the actual masses of the wall panels in question (cf. Fig. 3). Rather, equivalent (area-related) masses $m_1'^*$ and $m_2'^*$ are selected in such a way that the single-panel sound attenuation value R_1 (or R_2) is the same in the actual panel (with diffuse sound incidence) as in the model at vertical incidence when only the mass inertia is taken into account.

According to this definition, the following applies for determining $m_1'^*$ in a random panel :

$$R_1 \equiv 20 \lg \left[\frac{\pi f m_1'^*}{\varrho c} \right] \text{dB} \qquad (3)$$

in which R_1 represents the known sound attenuation of the first panel. The equivalent area weights $m_1'^*$ and $m_2'^*$ of the two panels result in:

$$m_1'^* = \frac{\varrho c}{\pi f} 10^{R_1/20} \qquad (4)$$

$$m_2'^* = \frac{\varrho c}{\pi f} 10^{R_2/20} \qquad (5)$$

These values lead to the double-panel attenuation R for this model according to equation (1):

$$R = R_1 + R_2 + 20 \lg \left[\frac{4 \pi f \varrho c}{s'} \right] \text{dB} \qquad (6)$$

for $f \gg f_R$

$$f_R = \frac{1}{2\pi} \sqrt{\frac{s' \pi f}{\varrho c} (10^{-R_1/20} + 10^{-R_2/20})} \qquad (7)$$

or specifically for two uniformly constructed panels with the attenuation factor R_1:

$$R = R_1 + 6 \text{ dB}, \qquad f \ll f_R \qquad (8)$$

$$R = 2 R_1 + 20 \lg \frac{4 \pi f \varrho c}{s'} \text{ dB}, \quad f \gg f_R \qquad (9)$$

$$f_R = \frac{1}{2\pi} \sqrt{\frac{2 \pi f s'}{\varrho c} 10^{-R_1/20}}. \qquad (10)$$

These expressions can be used when the values of attenuation R_1 and R_2 of the panels are known as a result of measuring. This is often the case, and thus R is easy to compute.

f_R, however, cannot be given explicitly, since R_1 depends on the frequency. Futhermore, R cannot be computed realistically in the vicinity of f_R, since the computation does not take into account the insulation. Therefore, the two solutions above and below f_R must suffice, and they have to be extended as an approximation to their point of intersection at f_R.

2.3 Approximation for limp panels

In the case of limp panels, where the critical frequency f_{gr} after Cremer (10) lies at the upper end of the frequency range in question, attenuation R_1 (or R_2) of the single panel after Heckl (5) can be approximated as follows for frequencies sufficiently below f_{gr}:

$$R_1 = 20 \lg \frac{\pi f m_1'}{\sqrt{2}\,\varrho c} \text{ dB}. \qquad (11)$$

The extended Wintergerst model can be used quantitatively when

$$m_1'^* = \frac{m_1'}{\sqrt{2}}, \quad m_2'^* = \frac{m_2'}{\sqrt{2}} \qquad (12)$$

is chosen.

The following applies to the double wall with equally heavy panels:

$$R = 20 \lg \frac{\pi f m_1'}{\sqrt{2}\,\varrho c} + 40 \lg(\sqrt{2}\, f/f_R) \text{ dB}, \qquad (13)$$

$$f_R = \frac{1}{2\pi} \sqrt{\frac{2\sqrt{2}\, s'}{m_1'}}. \qquad (14)$$

The difference compared with the previous Wintergerst approach above f_R is 6 dB. The resonance frequency increases by $\sqrt[4]{2}$.

2.4 Approximation for stiff panels

Above the critical frequency f_{gr} of the wall panels, the following applies to R_1 or R_2 according to Heckl (5):

$$R_1 = 20 \lg \left| \frac{\pi f m_1'}{\varrho c} \sqrt{2\eta} \sqrt[4]{f/f_{gr}} \right| \text{dB}. \quad (15)$$

In this, η represents the loss factor of the panel, f_{gr} its critical frequency. For the sake of simplicity, the following deals only with the case of two uniformly constructed panels. In that case, the following applies to attenuation factor R of the double wall:

$$R = 40 \lg \left(\frac{\pi f m_1'}{\varrho c} \sqrt{2\eta} \sqrt[4]{f/f_{gr}} \right) + \\ + 20 \lg \frac{4\pi f \varrho c}{s'} \text{dB} \quad (16)$$

the resonance frequency f_R results as follows:

$$f_R = \frac{1}{2\pi} \sqrt{\frac{2s'}{m_1'}} \sqrt[4]{\frac{1}{2\eta}}. \quad (17)$$

In this, one term $\sqrt[8]{f/f_{gr}}$ has been disregarded, which in a practical case would be about 1 in the various versions and would change very little. It can be seen from equation (17) that the resonance frequency equals the previous /p. 221 term of the Wintergerst model, although a multiplicative term $1/(\sqrt[4]{2\eta})$ is added. Depending on the magnitude of the loss factor η of the panels, which as a rule can be assumed to lie between 10^{-3} and $5 \cdot 10^{-3}$, this factor is about 3.2 or 4.7. Thus the previous computation of the resonance frequency of double-panelled walls with stiff panels has resulted in values which were 3 to 5 times too low.

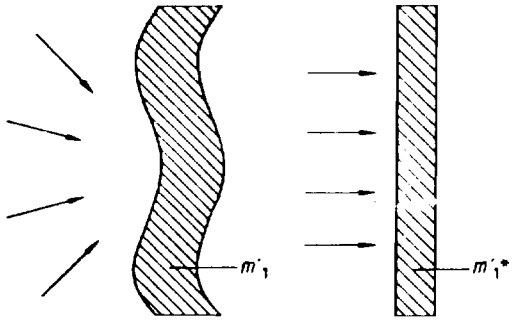

Fig. 3. Replacing the mass (per area unit) m_1' of the investigated wall panel with (reduced) mass $m_1'^*$ for the model after Fig. 1.

2.5 Improvement through facing-panels

The improvement Δ R of attenuation R of a randomly constructed panel or ceiling by means of a facing-panel (without rigid couplings) with attenuation factor R_1 results as follows after the above model:

$$\Delta R = R_1 + 20 \lg \frac{4 \pi f \varrho c}{s'} \text{ dB} \qquad (18)$$

for a limp facing-panel, the following is the approximate result:

$$\Delta R = 20 \lg \frac{4 \pi^2 f^2 m_1'}{V 2 s'} \text{ dB}. \quad f \gg f_R \qquad (19)$$

or

$$\Delta R = 40 \lg (f/f_R), \text{ dB}.$$

$$f_R = \frac{1}{2 \pi} \sqrt{\frac{V 2 s'}{m_1'}}. \qquad (20)$$

Apart from factor $\sqrt{2}$ at f_R, Cremer already arrived at this expression when he improved airborne sound attenuation by means of a floating floor (6). The following is assumed to apply to a stiff facing-panel:

for $f \gg f_R$

$$\Delta R = 40 \lg (f/f_R) + 5 \lg (f/f_{g,}) \text{ dB} \qquad (21)$$

$$f_R = \frac{1}{2 \pi} \sqrt{\frac{s'}{m_1'}} \sqrt[4]{\frac{1}{V 2 \eta}} \text{ dB}. \qquad (22)$$

By the way, formula (18) can also be applied accordingly to machine casings, where Δ R represents the reduction of the machine's noise level brought about by installing a casing. A condition is that s' is known for the cavity.

3. Stiffness of air layers

The dependence on the frequency of the dynamic stiffness s' of air layers will be discussed below; s' is defined as follows:

$$s' \equiv \left| \frac{p}{\xi} \right| \qquad (23)$$

p: sound pressure, ξ: vibration path of the panel.

For lower frequencies, the following known equation applies for a sufficiently attenuated air space with incident flexural waves:

$$s' = \frac{\varrho c^2}{d} \qquad (24)$$

c: velocity of sound in the air;
d: thickness of air layer.

It must be taken into account that because of the aerodynamic resistance brought into the air layer and because of the thus narrow thermal contact during the periodic fluctuations in pressure, the change cannot be adiabatic but must be isothermal. In case of an empty air layer - without introduced aerodynamic resistance - the stiffness with incidence of flexural waves in a panel is about five times greater; see (7) for details. For higher frequencies in which the tickness becomes comparable with $\lambda/2$ (λ wave length), it can be estimated for a case of an attenuated cavity if - as Wintergerst did for a cavity - only the sound propagation vertical to the cavity is taken into account; cf. diagram in Fig. 4. In this, stiffness s' refers to alternating pressure p ahead of the second wall panel.

Paths b and c depend on the length-specific aerodynamic resistance (θ) of the panel, the most favourable values at low frequencies being of no consequence, since they are valid only under the non-applicable condition that the material forming the aerodynamic resistance is so heavy that it does not move much under the influence of the alternating pressures.

At high frequencies ($d > \lambda/4$), the following can be assumed for stiffness s':

$$s' = 2\pi f \varrho c. \qquad (25)$$

/ p. 222

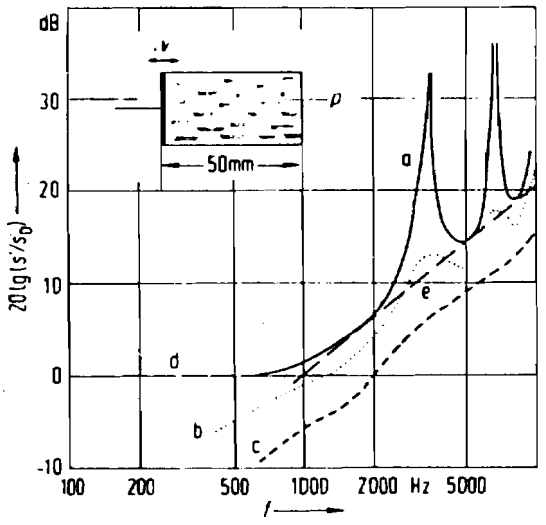

Fig. 4. Computed path of stiffness s' of an air layer in dependence of the frequency.

a: empty cavity,

b: length-specific aerodynamic resistance (θ) $=10^4$Ns/m^4,

c: (θ) $= 2\cdot10^4$Ns/m^4,

d,e: approximations.

In the case of deep cavities (d magnitude) and high aerodynamic resistance, s' will be smaller than stated. This factor, which means that the attenuation in a double wall is greater than the computed values indicate, will be disregarded below; see curve c in Fig. 4. The following can be assumed for double walls with air layers:

for low frequencies ($d \leq \lambda/4$):

$$s' = \varrho c^2/d$$

$$R = R_1 + R_2 + 20 \lg \frac{4\pi f d}{c} \text{ dB}, \qquad (26)$$

for high frequencies ($d > \lambda/4$):

$$s' = 2\pi f \varrho c$$

$$R = R_1 + R_2 + 6 \text{ dB}. \qquad (27)$$

In this connection it should be pointed out also that the attenuation minima resulting from the Wintergerst model (1), (4) of the air layer (without aerodynamic resistance) do not occur when the attenuation is measured.

In the case of an empty air space, the transverse modes of sound of the air layer (parallel to the attenuation minima) are so well defined that the

thickness resonance can be disregarded. In the attenuated cavity, the transverse modes and the thickness modes disappear. Thus, contrary to earlier views, attenuation of airborne sound in a double wall does not decrease when the thickness of the cavity is increased until $\lambda_L = 2\ d$.

4. Comparison between computed and experimental results

Below is a comparison between our computed results and results obtained experimentally with greatly varying double-panelled walls[1]. All of these are walls with completely separated panels, with mineral wool in the cavities (unless indicated otherwise) and measured spaces in which the flanking transmission was disregarded in favour of direct transmission.

In all cases, the following values were compared:

the experimental results (curve a),

the computed results (curve b) after expression (6) from experimentally known attenuation values of the single panels (curve e),

the results computed from expression (13) or (16) as curve c,

the results computed after Wintergerst, as curve d.

4.1 Limps panels

In Fig. 5, the results for a double wall of 12.5 mm plasterboard with a panel distance of 50 mm were compared in a very broad frequency range. Agreement between computed and experimental results was good in the lower frequencies. In the critical frequency, the computed results were too favourable. Above the boundary frequency, there is again relatively good agreement. This diagram clearly shows the varying behaviour in the range of limp panels at low frequencies and the stiff range above the critical frequency.

---

(1) Carried out at the Fraunhof Institute for Structural Physics in Stuttgart.

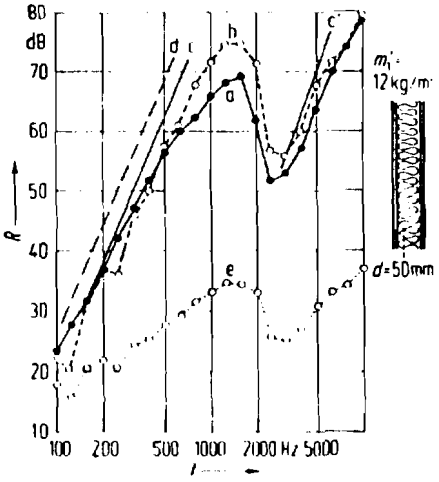

a: measured values,
b: computed acc. to expression 6,
c: approx. acc. to expression 13,
c': approx. acc. to expression 16,
d: after Wintergerst's expression (1),
e: measured values for attenuation factor R_1 of single panel.

Fig. 5. Attenuation of a double-panelled wall with panels made of 12.5 mm plasterboard (limp panels).

This shows that below and above the critical frequency of the panels. /p. 223 (about 3,000 Hz), two resonance frequencies must be differentiated which lie widely apart.. Understandably the range near the critical frequency cannot be defined by means of any of the two approximation solutions according to (13) or (16). But it is possible to compute according to (7) from the experimental values for R_1 ($R_1 = R_2$ for panels of uniform construction). The deviation of this computation from the results in the vicinity of the critical frequency cannot be disregarded. But in a practical application, even such an approximation would be welcome.

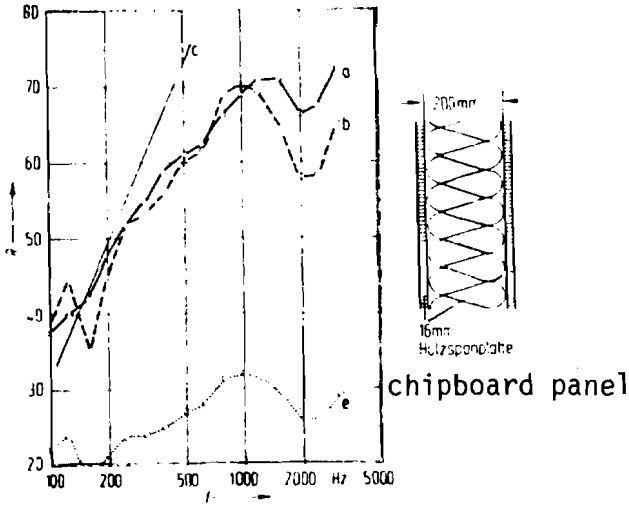

chipboard panel

Fig. 6. Attenuation of a double-panelled wall made of 16 mm chipboard, with a panel distance of 200 mm. Key: same as Fig. 5.

Fig. 6 shows a wall with a very wide distance between panels (200 mm). In this case, the computed results in the vicinity of the trace-fitting frequency are too low in comparison with experimental results. The probable reason is that the noise level reduction in the cavity from one panel to another, resulting from the aerodynamic resistance, has been disregarded.

4.2 Stiff panels

For these, we first took results from the literature (8) for a double wall of 80 mm plasterboard (see Fig 7). In this case, too, there is satisfactory agreement between the experimental results and those computed from R_1 (which was also measured). Fig. 7, curves c and c_1 show the boundaries of a direct computation from material data according to expression (16). When a loss factor $\eta = 6 \cdot 10^{-3}$ is used for plasterboard, as the literature (9) suggests, agreement is unsatisfactory (curve c). Good agreement could only be achieved with a loss factor $\eta = 10^{-3}$ (curve c_1). In the present case, the single wall, too, showed a particularly low attenuation compared with other empirical values. Thus, in this specific arrangement, a low loss factor is probable.

Fig. 8, finally, shows the case of a double-panelled dividing-wall between two houses, with an interspace running along the entire length of the houses. The insulation layer in the interspace consisted of 20 mm hard-foam boards, the walls consisted of 100 mm concrete slabs. In this case, measurements were taken in a dividing-wall between two houses under construction. The stiffness of the insulation layer could only be estimated, because in such insulation layers ($E \approx 300$ MN/m^3) the thickness of the air layer between insulation layer and wall panel is not exactly known, although this thickness determines s'. It was assumed to be 2 mm, and the total stiffness of the insulation layer including the air layer was assumed to be 50 MN/m^3.

There is satisfactory agreement between computation (7) and measured results, particularly when compared with the results according to the old Wintergerst model after expression (1), curve d. The computation according to (16) also gives good agreement, provided that a loss factor $\eta = 5 \cdot 10^{-3}$ is used, as has been the case in the literature (9): ($\eta = 4 - 8 \cdot 10^{-3}$).

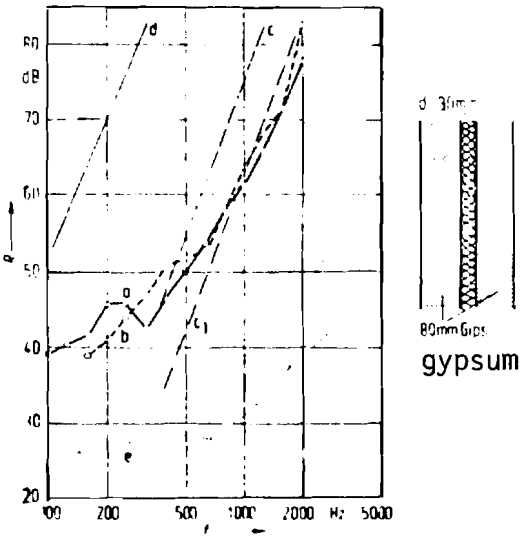

Fig. 7. Attenuation of a double-panelled wall made of 80 mm plasterboard (stiff panels).
Key: same as in Fig. 3.
c_1: simplified computation according to (16) for loss factor $\eta = 10^{-3}$,
c: $\eta = 5 \cdot 10^{-3}$.

In summary this leads to the conclusion that in the case of stiff / p. 224 panels the computation should be based on the experimental values R_1 of the single panels, since the material attenuation measured in small individual samples in the laboratory for the loss factor η of the entire wall is not the only factor: there is also transmission via lateral constructions, and this renders the computation unreliable.

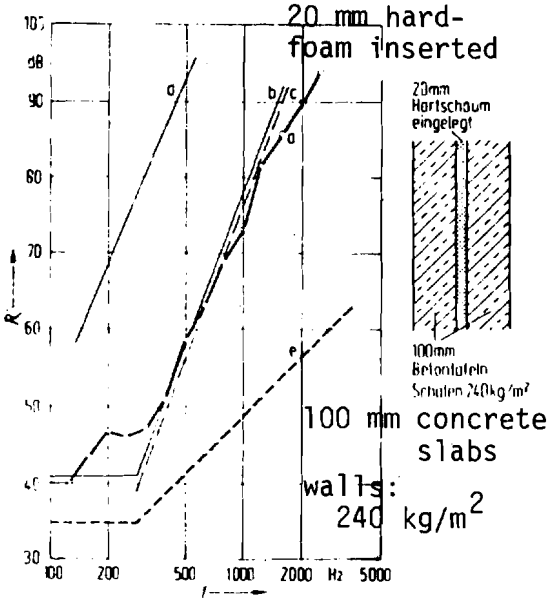

Fig. 8. Attenuation R' of a double-panelled dividing-wall between houses, with completely separated walls made of 100 mm concrete slabs, with 20 mm hard-foam boards in the interspaces, measured during construction.
a: experimental results,
b: computed results after expression (6), from values for R_1 (see e),
c: computed results after expression (6),
d: after the original Wintergerst formula (1),
e: single-panelled wall after empirical values (12).

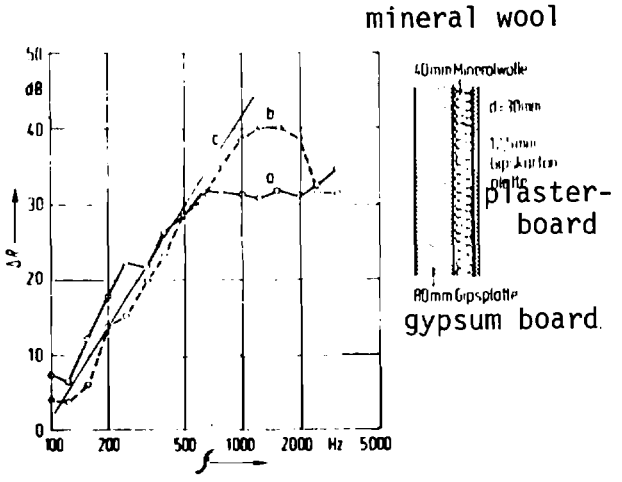

Fig. 9. Improvement Δ R of the attenuation of a solid wall by means of a limp flexible facing-panel.

a: experimental results,

b: computed after (18) from the attenuation R_1 of the facing-panel,

c: simplified computation after (20).

4.3 Improvement through facing-panels

This will be discussed in relation with two cases: a limp and a stiff facing-panel.

Fig. 9 shows experimental results of improvement Δ R for a facing-panel made of 12.5 mm plasterboard attached to a wall made of 80 mm plasterboard in a laboratory, with suppressed flanking transmission. In the lower and intermediate frequencies, computed and experimental results agree satisfactorily; the same is true in the case of computation after (18), using the experimental R_1 values of the plasterboard panels (curve b) as well as in the case of the simplified computation after expression (20), line c.

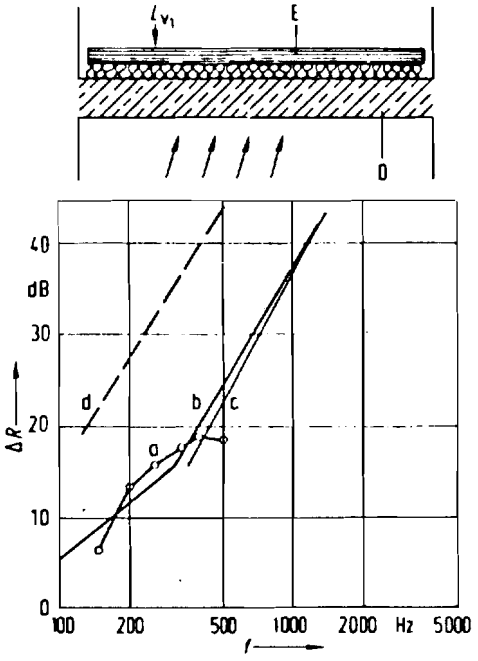

Fig. 10. Improvement Δ R in the attenuation of a ceiling D by means of a floating floor E (stiff panel) over 20 mm mineral fibre board.
a: experimental results (from sound level L_{vo} and L_{v1}),
b: computed results after (18),
c: simplified computation after (21),
d: computed results after the old Wintergerst model.

The deviation in higher frequencies may result on the one hand from the limited longitudinal insulation of the test stand, on the other hand from the possible presence of very minor couplings between facing-panel and solid wall.

As our second case, the improvement of airborne sound attenuation by means of a floating floor will be discussed (Fig. 10). In this case, direct measuring of the airborne sound attenuation was not possible because of flanking /p. 225
transmission which was a disturbance factor even in the laboratory. For that reason, we measured the velocity level of the floating floor (L_{v1}) and of the ceiling without floating floor (L_{vo}), and from this we determined the airborne sound attenuation and the improvement Δ R as a result of the floating floor. However, below the critical frequency of the floating floor (about 300 Hz), this determination is very inaccurate. Actually, the amount of sound radiation emitted by the floating floor would have to be taken into account,

but because free as well as forced flexural waves occur, this amount cannot be computed with accuracy. The computation after (18) was based on attenuation factor R_1 of an appropriate concrete slab after Heckl (12).

5. Direct computation of airborne sound attenuation (without model)

The previous computation was based on a spring-mass model in which the masses of the model were chosen in such a way that under the influence of the sound pressure and assuming pure mass inertia, they have the same vibration amplitudes as the actual wall with its flexural vibrations.

We will now attempt to compute the attenuation of a double wall without reference to a model. This is based on a diffuse sound field with sound pressure p_1, at the double wall in question (see Fig. 11), and on the following two assumptions:

(a) that sound pressure p_H in the wall cavity can be computed from sound pressure p_1 in the source room and from the attenuation factor R_1 of the first panel;
(b) that the radiated sound energy of the second panel can be computed from p_H, the attenuation factor R_2 and wall area S.

ad (a): The following applies when the aerodynamic resistance in the wall cavity is sufficiently great:

$$p_H = \frac{s' v_1}{2\pi f}, \qquad (28)$$

v_1 is computed from

$$R_1 = 20 \lg \frac{1/2\, p_1}{\varrho c v_1} \text{ dB}. \qquad (29)$$

In this it is assumed that v_1 is not the true vibration velocity of the panel but a mean value of those portions whose flexural wave length

is $\lambda_B \geq \lambda_L$.(2) Thus,

:

$$p_H = \frac{s' 1/2\, p_1\, 10^{-R_1/20}}{2\pi f \varrho c} \quad . \qquad (30)$$

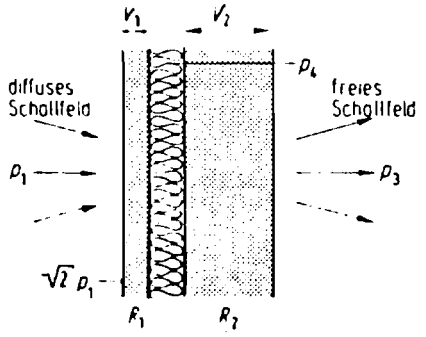

Fig. 11. Computing sound attenuation in a double wall.

Key: 1. diffuse sound field,
2. free sound field.

ad (b): For the sake of simplicity it is assumed that attenuation factor R_2 for the second panel results in about the same way if on the one hand the panel is subject to sound pressure p_H in the cavity or on the other hand to the equally intense sound pressure $p\sqrt{2}$ of a diffuse sound field of a room with sound pressure p.

This assumption is probably not quite correct. Thus, a correction factor k is applied as well:

$$R_2 = 20 \lg \frac{p_H}{\sqrt{2}\, p_3} + 10 \lg \frac{S}{A} + k \text{ dB} . \qquad (31)$$

A deviation can be expected because the trace wavelengths of the pressure distribution at the second panel are distributed differently in the cavity than in a case where the diffuse sound field is directly incident on the panel. The definition equation for the attenuation factor R of the double-panelled wall

---

(2) Translator's note: The footnote seems to be out of place. The first line reads: Carried out in the Fraunhofer Institute for Structural Physics. The second and subsequent lines read: ... parts ... in an attenuated cavity can also supply a portion of sound pressure p_H, but cannot lead to any sizeable transmission and can therefore be disregarded.

$$R = 20 \lg \frac{p_1}{p_2} + 10 \lg \frac{S}{A} \text{ dB} \qquad (32)$$

together with (30) results in

$$R = R_1 + R_2 + 20 \lg \frac{4 \pi f \varrho c}{s'} - k + 3 \text{ dB}. \qquad (33)$$

6. Comparison with the modified Wintergerst model

The computation based on the modified Wintergerst model, see expression (6), results in an attenuation factor R that is 3 dB lower than the computation outlined here, if k = 0. This deviation is caused by the fact that the model according to Fig. 1 uses vertically incident sound, while the computation /p. 226 discussed above is based on the diffuse sound field of a source room. Incidentally, this deviation occurs because the attenuation factor R is inadequately defined in physics (as a ratio between two sound energies), as Rindel explained in detail. This deficiency could be remedied by basing the model on obliquely incident sound as well.

The question remains as to the magnitude of the empirically introduced constant k in expression (33). For this, Fig. 12 shows the difference between the computation according to expression (33) for k = 0, and the measured results for a double wall according to Fig. 5, dependent on the frequency (Translator's note: The last part of this sentence and all but one word of the following sentence are missing).... plot. It represent k. Thus k lies roughly between 0 and 10 dB. The maximum deviation occurs somewhat below $f/f_{gr} = 1$. It can be expected that this path depends on the dimensions of the wall in question, in relation to wavelength λ_{gr} at the critical frequency, as is the case, too, with the attenuation of sound in single-panelled walls.

In summary, the following conclusions can be drawn from this:

(a) The above mentioned correction of 3 dB in the computation according to Wintergerst's model should not be used, since this would increase the maximum errors between model computation and experimental results.

The model computation then applies to k = 3, see line a in Fig. 12.

(b) In stiff panels ($f_{gr} < f$), the expected deviations are probably relatively minor in terms of the model computation, because the relevant values will for the most part lie above the critical frequency.

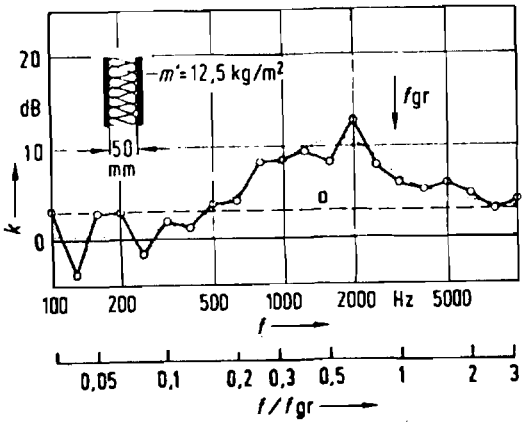

Fig. 12. Correction factor k, determined from experimental results according to Fig. 5, for wall panels with f_{gr} = 3,000 Hz and measuring 2.5 m x 3 m.
a: correction already included in the modified Wintergerst model.

(c) In the vicinity of $f = f_{gr}$, the deviations are highest, and the errors probably seldom exceed 7 dB (in terms of line a) as was the case here, since the dimensions of λ_{gr} are particularly large in this example.

7. Final conclusions

Sound attenuation in double-panelled constructions -without rigid couplings between the panels and with an insulated cavity- can be computed in advance according to an improved mass-spring-mass model. Two different computation methods can be used:

(a) It is assumed that the values of attenuation factor R_1 and R_2 of the two panels are known. Then, the computation is possible in the entire frequency range. The following attenuation factor R of the double wall results above the resonance frequency:

$$R = R_1 + R_2 + 20 \lg \frac{4 \pi f \varrho c}{s'} \text{ dB} \qquad (6)$$

in which s' is the dynamic stiffness of the insulation layer between the panels.

(b) The attenuation can also be computed directly from the material data of the panels; this computation is possibly only sufficiently below or above the critical frequency of the panels. The following applies in the case of two uniformly made limp panels:

$$R = 20 \lg \left(\frac{\pi f m'}{\sqrt{2}\, \varrho c} \right) + 40 \lg \frac{\sqrt{2} f}{f_R} \text{ dB}$$

$$f_R = \frac{1}{2\pi} \sqrt{2\sqrt{2}\, \frac{s'}{m_1'}} \qquad (13)$$

in the case of two uniformly made stiff panels:

$$R = 40 \lg \left(\frac{\pi f m_1'}{\varrho c} \sqrt{2\eta} \sqrt{f/f_{gr}} \right) +$$

$$+ 20 \lg \frac{4\pi f \varrho c}{s'} \text{ dB}. \qquad (16)$$

Solution (a) is preferable unless the panels are limp. With stiff panels the solution in accordance with (b) depends on often uncertain assumptions regarding the magnitude of loss factor η of the wall panels.

A comparison between computed and experimental results using a great variety of panels and panel distances leads to agreement that is sufficient for practical purposes. Major deviations can occur only in the vicinity of the critical frequency. /p. 227

The computation method can also be used to improve ΔR of sound attenuation through facing-panels, floating floors and machine casings.

Received for publication: Jan. 17, 1980.

Literature cited

[1] Wintergerst, E., Theorie der Schalldurchlässigkeit von einfachen und zusammengesetzten Wänden. Schalltechnik 4 [1931], 85 und 5 [1932], 1.

[2] London, A., Transmission of reverberant sound through double walls. J. Acoust. Soc. Amer. 22 [1950], 270.

[3] Cops, A., Mynke, H. und Vermeir, G., Insulation of reverberant sound through double and multilayered glass constructions. Acustica 33 [1975], 258.

[4] Cremer, L., Vorlesungen über Technische Akustik. Bild 20.5.

[5] Heckl, M., Die Schalldämmung von homogenen Einfachwänden endlicher Fläche. Acustica 10 [1960], 98.

[6] Cremer, L., Näherungsweise Berechnung der von einem schwimmenden Estrich zu erwartenden Verbesserung. In: Fortschritte u. Forschungen im Bauwesen, Reihe D, Heft 2, [1952], 121.

[7] Gösele, K. und Gösele, U., Einfluß der Hohlraumdämpfung auf die Steifigkeit von Luftschichten bei Doppelwänden. Acustica 38 [1977], 159.

[8] Gösele, K., Der Einfluß der Biegesteifigkeit auf die Schalldämmung von Doppelwänden. Acustica 4 [1954], 276.

[9] Cremer, L. und Heckl, M., Körperschall. Springer-Verlag, Berlin 1967.

[10] Cremer, L., Theorie der Schalldämmung dünner Wände bei schrägem Einfall. Akust. Z. 7 [1942], 81.

[11] Rindel, J. H., Transmission of traffic noise through windows. The Acoustics Laboratory, Techn. University of Denmark, Report Nr. 9, 1975.

[12] Heckl, M. und Müller, H. A., Taschenbuch der Technischen Akustik. Springer-Verlag, Berlin 1975, p. 440, Springer-Verlag, Berlin 1971, 285 - 289.